

Design and Control of Single-stage LED Converter with High Power Factor

Geun-Yong Park and Gang-Youl Jeong*

Soonchunhyang University
*gangyoul@sch.ac.kr

Abstract

This paper presents a single-stage LED converter with high power factor. The proposed converter utilizes a single-stage power circuit that combines the boost DC-DC converter topology and the flyback converter topology. The control of the proposed converter operates using critical conduction mode and fixed on-time voltage control techniques. In this way the proposed converter is much simpler than current conventional LED converters. An operational principle and a design example of the proposed converter are explained, briefly. Also, it is shown through experimental results that the proposed converter built based on the design example has good performance for driving LEDs.

Keywords: *Single-stage, LED converter, high power factor, critical conduction mode, fixed on-time*

1. Introduction

As light-emitting diodes (LEDs) have many advantages such as small size, high luminous efficiency, long lifetime, fast response, and excellent color rendering, they have been widely used in many lighting applications. LEDs are environmentally friendly devices compared with conventional fluorescent lamps that require mercury and may produce pollution. Therefore, in pursuit of energy-saving and pollution free light sources, LEDs have gradually replaced fluorescent lamps and have become increasingly and more widely used [1-8].

As switching-mode AC-DC converters have many advantages such as high energy-conversion efficiency, high power density, and high control accuracy, they have been adopted as LED-driving converters that use a utility AC input. Conventionally, an AC-DC converter uses a bridge-diode rectifier and a bulky capacitor to obtain a nearly constant DC-link voltage for the next high-frequency DC-DC converter stage. Such an LED converter inevitably introduces a highly distorted AC input current due to the large amount of harmonics resulting in a low power factor. To comply with the stringent regulation on current harmonics such as IEC-61000-3-2 class C and to improve the power factor, an additional AC-DC conversion stage is needed to cascade in front of the DC-DC converter to perform the function of power factor correction (PFC). This leads to a double-stage approach which is composed of a PFC stage to make the input current sinusoidal and a DC-DC conversion stage to regulate the output voltage [9-11].

The double-stage approaches have advantages in that it can easily obtain a high power factor and low harmonic distortion, also they can be designed optimally to include enough time for energy accumulation. However, because the double-stage approaches utilize independent controllers for the PFC stage and the DC-DC converter stage, its control circuit becomes complicated, and thus their implementation cost is high. Also, because they must process

power-conversions twice, their total efficiency is lower. Recently, many single-stage AC/DC converters have been developed [12-16].

The single-stage approaches have been derived by merging the boost DC-DC converter and the flyback converter. By sharing one active power switch and the control circuit, the single-stage approaches have advantages such as a simple circuit configuration, ease of control implementation and are cost-effective solution. Therefore, recently, the single-stage approaches for driving of LEDshav been widely utilized in general lighting applications.

In this paper, a single-stage LED converter with high power factor is presented. A DC-DC boost converter and a flyback converter are combined into a single-stage power conversion circuit. The proposed converter is controlled using the critical conduction mode technique and the fixed on-time voltage control technique. Therefore the total circuit of the proposed converter is very simple and small. The proposed converter offers a high power factor, high efficiency, cost-effectiveness, and constant output voltage/current. In this paper, an operational principle and a design example of the proposed converter are described, briefly, and experimental results of a prototype are shown. A 32-W prototype converter has been built based on the design example and tested to show the feasibility of the proposed converter. The prototype shows very good performance.

2. Operational Principle of the Proposed Converter

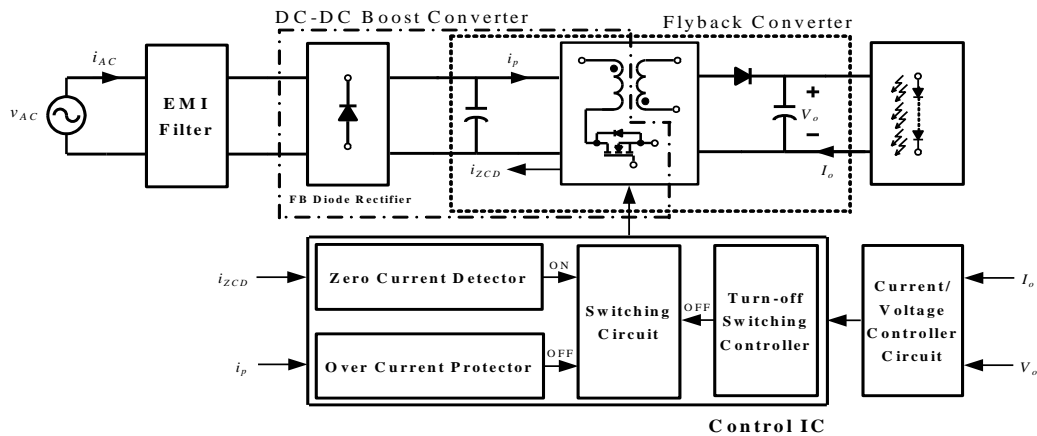


Figure 1. Conceptual Block Diagram of the proposed Converter

Figure 1 shows a conceptual block diagram of the proposed converter. The proposed converter is composed of a power circuit and a control circuit. The power circuit includes an electro-magnetic interference (EMI) filter, Full-bridge (FB) diode rectifier, single-stage converter, and LED load. The single-stage converter is a merged converter which comprises the DC-DC boost converter and the flyback converter. As the proposed converter uses a single-stage power topology, it can be simplified. The flyback converter operates with high frequency and controls the power flow using only one power semiconductor switch. This allows miniaturization and a lightweight construction. However, the AC input current of the flyback converter without any measures includes many harmonics due to the nonlinear operation of the FB diode rectifier connected at the AC input stage, as such the rectifier deteriorates the total harmonic distortion (THD). In order to overcome these shortcomings, the proposed converter owns a transformer and power semiconductor switch jointly and connects the DC-DC boost converter in front of the flyback converter. Thus the proposed converter achieves a single-stage converter structure. The proposed converter is simpler than

conventional LED converters, which are generally double-stage converters composed of a PFC stage and a DC-DC buck converter stage. So implementation costs are lower and it is simpler than conventional double-stage converters.

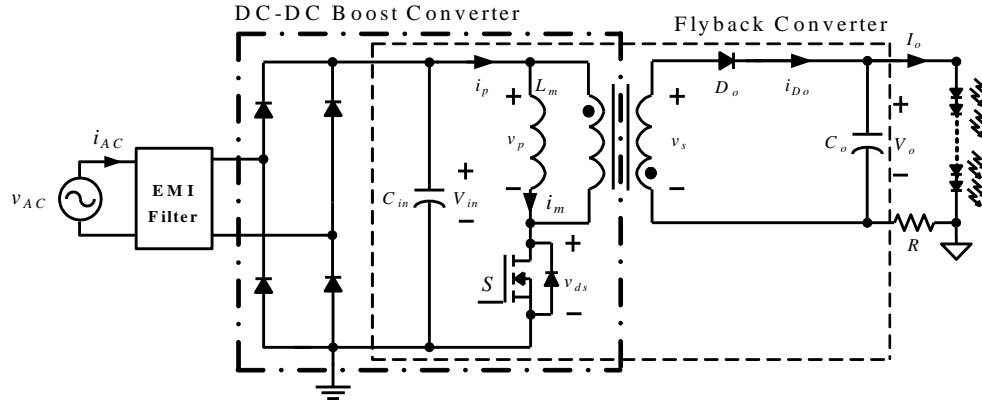


Figure 2 The Main Power Circuit of the proposed Single-stage LED Converter.

Figure 2 shows the main power circuit of the proposed single-stage LED converter, and Figure 3 shows the theoretical waveforms of the key parts of the proposed converter.

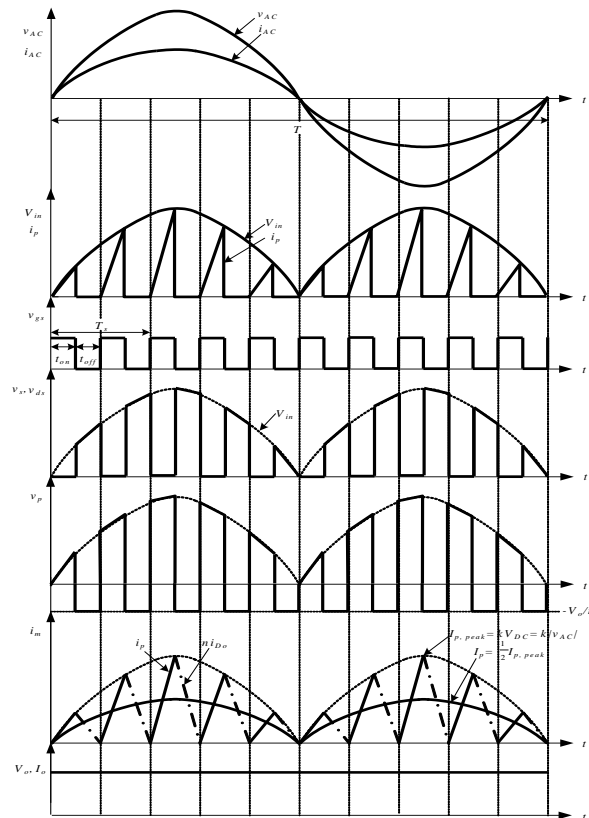
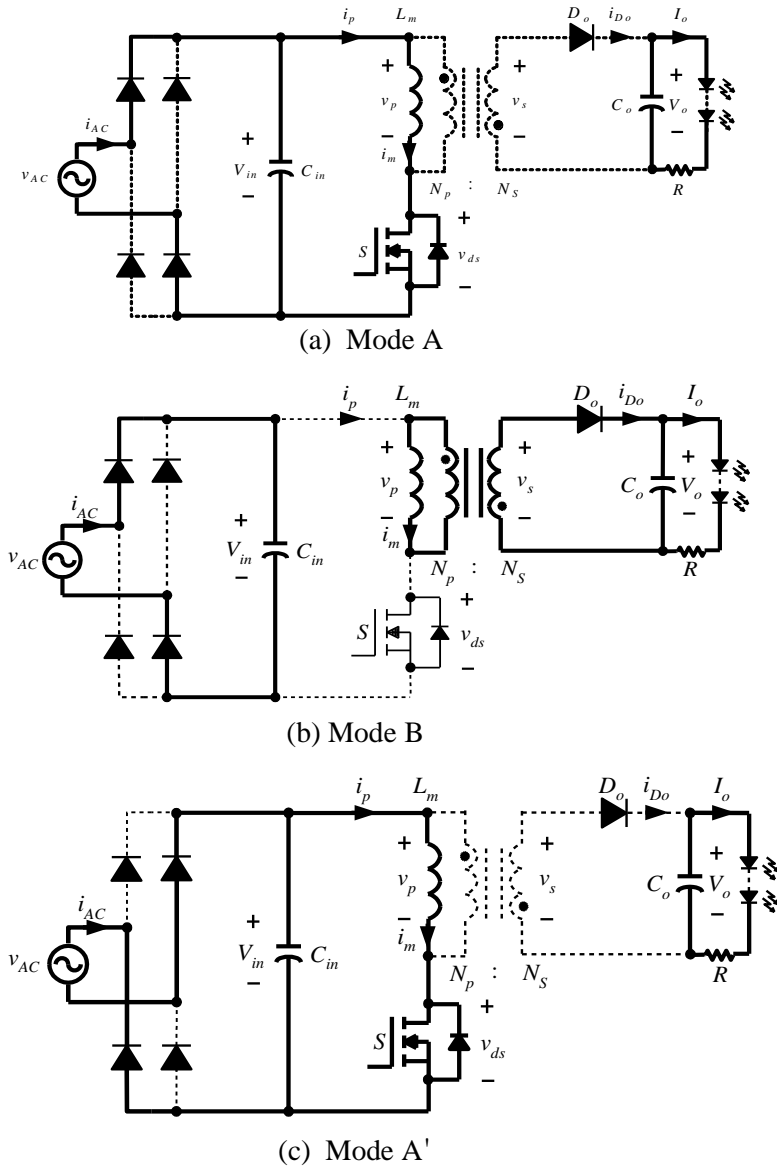
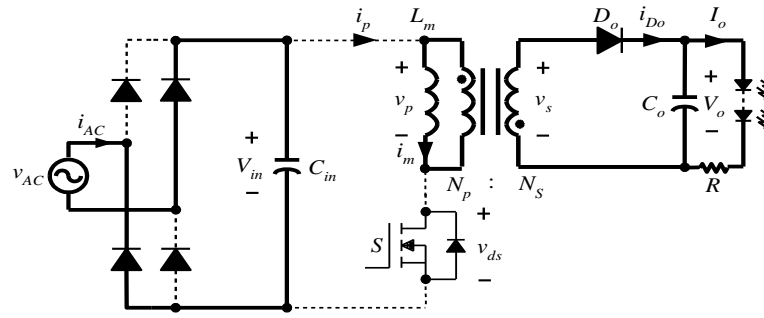


Figure 3 The Theoretical Waveforms of the Key Parts of the proposed Converter

Also, the proposed converter operates in critical conduction mode (CCM). This is different from the conventional single-stage LED converters that operate in either continuous conduction mode or discontinuous conduction mode. The proposed converter operating with the CCM has an advantage in that it can achieve zero-voltage switching (ZVS) without any additional active snubber circuit. Other advantages include a lower THD of the line current, lower turn-off switching losses, and lower conduction losses due to a smaller peak inductor current when compared with conventional single-stage LED converters [17].





(d) Mode B'

Figure 4 The Operation Modes of the proposed Single-stage LED Converter

Figure 4 shows the operation modes of the proposed single-stage LED converter, where the bold line represents the conduction line and the dotted line represents the no conduction line. Before the operation mode analysis, the following assumptions are made for the proposed converter:

- The switching frequency of the main power semiconductor switch is much higher than the AC input voltage frequency. Therefore the AC input voltage is considered to be constant at the switching instant.
- The output capacitance C_o is large enough that the output voltage V_o is a constant value.
- As EMI filter is considered ideal, as a matter of convenience for analysis, it is omitted.

Mode A ($t_0 \sim t_1$)

When the switch S turns on at time $t=t_0$, this mode starts. The AC input voltage ($v_{AC}=V_m \sin(2\pi f)t=V_m \sin\omega t$) at a positive half cycle is presented directly through the FB diode rectifier and charges the input capacitor C_{in} , and thus the AC input voltage equals the rectified DC voltage. Then, the primary current i_p or switch current that equals the magnetizing current i_m through the magnetizing inductance L_m and charges it. Therefore the primary current i_p is calculated as follows:

$$v_{AC} = V_{in} = v_p = L_m \frac{di_p}{dt} \quad (1)$$

$$i_p(t) = i_m(t) = \frac{1}{L_m} \int_{t_0}^t V_{in} d\tau. \quad (2)$$

As the AC input voltage is considered to be constant at the switching instant and the proposed converter operates with CCM, i_p is calculated as follows:

$$i_p(t) = i_m(t) = \frac{V_{in}}{L_m} (t - t_0). \quad (3)$$

At time $t=t_1$, the primary current i_p reaches its peak value $I_{p,peak}$ as follows:

$$I_{p,peak} = i_p(t_1) = i_m(t_1) = \frac{V_{in}}{L_m} (t_1 - t_0) \cong \frac{\Delta t}{L_m} V_m \sin\omega t_1 \quad (4)$$

where $\Delta t=t_1-t_0$.

In this mode, the secondary output capacitor C_o discharges power to the load. When the switch S turns off at time $t=t_1$, this mode ends.

Mode B ($t_1 \sim t_2$)

When the switch S turns off at time $t=t_1$, this mode starts. The primary current i_p becomes zero. If the secondary diode D_o is turned on, the primary voltage v_p becomes –

$N_p V_o / N_s$. Then the magnetizing current i_m decreases linearly, and the energy in the magnetizing inductance L_m is discharged to the transformer secondary. The magnetizing current i_m is given as follows:

$$\frac{di_m}{dt} = -\frac{V_o}{nL_m} \quad (5)$$

$$i_m(t) = \frac{1}{L_m} \int_{t_1}^t \left(-\frac{V_o}{n}\right) d\tau = -\frac{V_o}{nL_m} (t - t_1) + I_{p,peak} \quad (6)$$

where $n = N_s / N_p$ is the turn ratio of the transformer.

When the switch S turns on at time $t = t_2$, this mode ends.

If the AC input voltage is in a negative half cycle (modes A' and B'), the rectified DC input voltage V_{in} is the same as when the AC input voltage is at a positive half cycle due to the operation of the FB diode rectifier ($V_{in} = |v_{AC}|$). Therefore, the operations of the converter at a negative half cycle are also the same as in modes A and B. Thus, the analysis of modes A' and B' in a negative half cycle of the AC input voltage is omitted.

3. Power Factor Analysis of the Proposed Converter

In the proposed converter, the primary current i_p is conducted by the rectified DC input voltage V_{in} of the AC input voltage v_{AC} ($V_{in} = |v_{AC}|$) and is given by (3). The time function type $i_{p,peak}(t)$ of the primary peak current $I_{p,peak}$ can be approximated and induced from (4) as follows:

$$i_{p,peak}(t) \cong \frac{\Delta t}{L_m} V_m |\sin \omega t| = k V_m |\sin \omega t| \quad (7)$$

where $k = \Delta t / L_m$, and $\Delta t = t_1 - t_0$, from (4) and figures 3 and 4, is the nominal switch on time that is set by the peripheral circuit of the control IC in figure 1. The nominal switch on time Δt is a constant value and is determined according to the magnetizing inductance L_m , the minimum AC input voltage $v_{AC,min}$, and the maximum output power $P_{o,max}$.

The average value $I_p(t)$ of the primary current i_p during the switching period is calculated by the following equation:

$$I_p(t) = \frac{t_{on}}{T_s} \times \frac{1}{2} \times i_{p,peak}(t) = \frac{1}{2} D k V_m |\sin \omega t| \quad (8)$$

where $D = t_{on} / T_s$ is the turn-on duty, and the switching period T_s is the summation of the switch turn-on time t_{on} and the switch turn-off time t_{off} ($T_s = t_{on} + t_{off}$).

However, as shown in figure 1, the switch turn-off time t_{off} is determined by the operation of the turn-off switching controller in the control IC according to the output of the voltage controller circuit that is a PI (Proportional-Integral) controller. In general, because the PI controller is stable and can make the control object converge to its reference value, the output of the voltage controller is converged to its reference value and becomes nearly constant in a steady state. Therefore the switch turn-off time t_{off} becomes a nearly constant value, and thus the switching period T_s also becomes nearly constant. It follows that the turn-on duty ratio D also becomes a nearly constant value, and the average primary current $I_p(t)$ in the switching period can be rewritten as follows:

$$I_p(t) = K V_m |\sin \omega t| \quad (9)$$

where $K = Dk/2$ is a nearly constant value.

If the EMI filter at the AC input in figure 1 is connected and operated correctly, from (9) the AC input line current i_{AC} at the AC line frequency by the FB diode rectifier becomes as follows:

$$i_{AC} = K V_m \sin \omega t \quad (10)$$

Therefore, it can be known that the AC input voltage and current become in-phase and thus the power factor of the proposed converter becomes unity.

4. Design of a Prototype Converter

To validate the feasibility of the proposed LED converter, a prototype converter was designed with the following specifications:

- AC input voltage: $v_{AC}=90\text{-}265\text{ V}$, 60 Hz
- Maximum output power: $P_{o,\max}=32\text{ W}$ ($V_o=40\text{ V}$, $I_{o,\max}=800\text{ mA}$)
- Nominal minimum switching frequency at a minimum AC input voltage: $f_{s,\min}=50\text{ kHz}$
- Nominal turn-on duty at a maximum output current: $D_{nom}=0.45$

As the switching frequency f_s is much higher than the AC input line frequency, the AC input current i_{AC} during one switching period is assumed to be constant. The maximum AC input current $I_{AC,\max}$ is calculated by the following equation:

$$I_{AC,\max} = \frac{\sqrt{2}P_{o,\max}}{\eta v_{AC,\min}} = \frac{\sqrt{2} \times 32}{0.82 \times 90} = 613\text{ mA} \quad (11)$$

where η is the design efficiency and is set to 82% ($\eta = 0.82$) in this design. The maximum switch or primary current $I_{p,\max}$ is given by the following equation:

$$I_{AC,\max} = \frac{1}{T} \int_0^{DT_s} \frac{I_{p,\max}}{DT_s} t dt = \frac{D}{2} I_{p,\max} \quad (12)$$

$$I_{p,\max} = \frac{2}{D} I_{AC,\max} = \frac{2}{0.45} \times 0.613 = 2.72\text{ A} \quad (13)$$

where D is set to the nominal turn-on duty ($D=D_{nom}=0.45$) at maximum output current.

The transformer primary voltage v_p is given as follows:

$$v_p = L_m \frac{\Delta i}{\Delta t} \cong L_m \frac{I_{p,\max}}{DT_{s,\min}} \quad (14)$$

Therefore, from (12) and (13), the magnetizing inductance L_m is calculated as:

$$L_m \geq \frac{D^2 \cdot \sqrt{2} v_{AC,\min}}{2 I_{AC,\max} f_{s,\min}} = \frac{0.45^2 \times \sqrt{2} \times 90}{2 \times 0.613 \times 50 \times 10^3} \cong 420\text{ }\mu\text{H}. \quad (15)$$

Then, the magnetizing inductance L_m is set as 480 μH . The turn number of the transformer's primary winding can be calculated using the following physical inductance equation:

$$L_m = \frac{N^2}{R_m} = \mu_m N^2 \quad (16)$$

where R_m is the reluctance of the transformer core, and μ_m is the core's permeability or the reciprocal of reluctance R_m . In this design, μ_m was selected to be 240 nH/N², which is the permeability of the transformer core EFD 3030 used in this prototype converter. Thus, the turn number of the transformer's primary winding is calculated as $N_p=45$. Also, the turn number of the transformer's secondary winding can be calculated using the voltage-transfer ratio equation of the conventional flyback converter and was selected as $N_s=18$. So the turn ratio of the transformer n becomes $n=N_s/N_p=18/45=0.4$.

When the switch S is turned off, voltage stress is applied to the switch due to the flyback operation of the converter. Thus, the maximum voltage stress $V_{ds,\max}$ of the switch S is considered as the following equation:

$$V_{ds,\max} = \frac{V_o}{n} + \sqrt{2} v_{AC,\max} = \frac{40}{0.4} + \sqrt{2} \times 265 = 475\text{ V} \quad (17)$$

Therefore, the switch S was selected as a 600-V/12-A commercial MOSFET.

In the design of the secondary output diode D_o , the reverse voltage V_{DR} and forward peak current $I_{D,\text{peak}}$ of the diode are considered. These specifications of the output diode are calculated by the following equations:

$$V_{DR} = V_o + n\sqrt{2} v_{AC,\max} = 40 + 0.4 \times \sqrt{2} \times 265 \cong 190\text{ V} \quad (19)$$

$$I_{D,\text{peak}} = \frac{2}{1-D} I_o = \frac{2}{1-0.45} \times 0.8 \cong 2.9\text{ A} \quad (20)$$

Thus, the diode D_o was selected as a 400-V/10-A commercial diode.

5. Experimental Results

To validate the feasibility of the proposed LED converter, a prototype converter, based on the design example in Section 4, was constructed and tested.

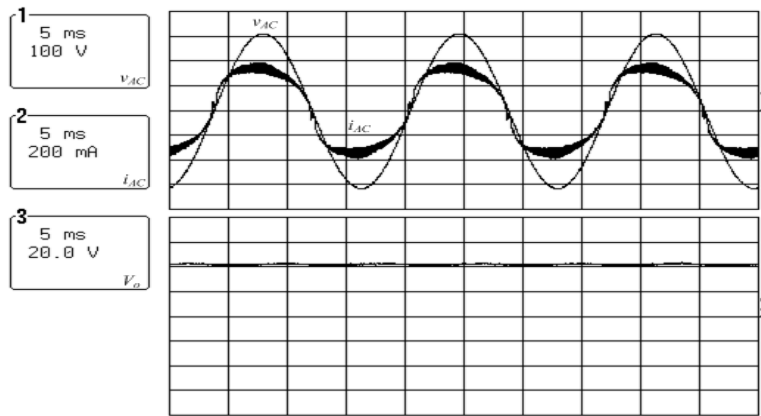
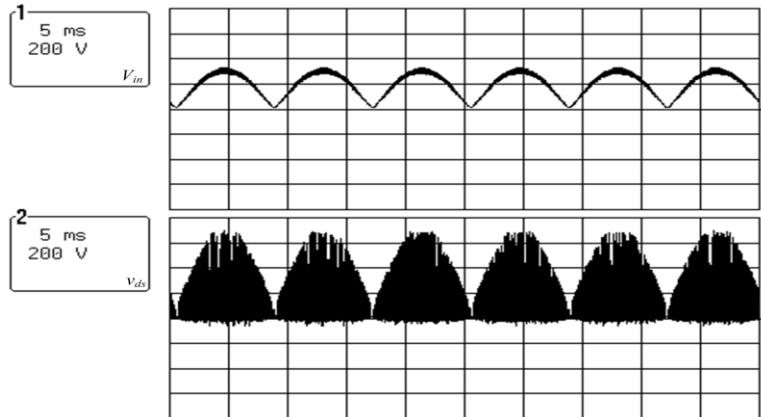


Figure 5 The Experimental Waveforms of the AC Input Voltage and Current, and the DC Output Voltage and Current of the proposed LED Converter

Figure 6 The Experimental Waveforms of the Key Parts of the proposed



Converter at a line Frequency Scale

Figure 5 shows the experimental waveforms of the AC input voltage and current, and the DC output voltage and current of the proposed LED converter. These waveforms show that the power factor of the proposed converter is nearly unity, and the proposed converter can maintain a constant output voltage and current for constant brightness of an LED.

Figure 6 shows the experimental waveforms of the switch voltage v_{ds} and the rectified DC input voltage V_{in} of the proposed converter at a line frequency scale. These waveforms show that the control IC with the CCM control function operates very well for driving the proposed flyback converter, and the proposed converter circuit is well designed and operates well.

Figure 7 shows the experimental waveforms of the PWM output v_{gs} of the control IC and the switch voltage v_{ds} of the proposed converter at a switching frequency scale. These waveforms show that the control IC of the proposed converter correctly drives the main switch of the proposed converter.

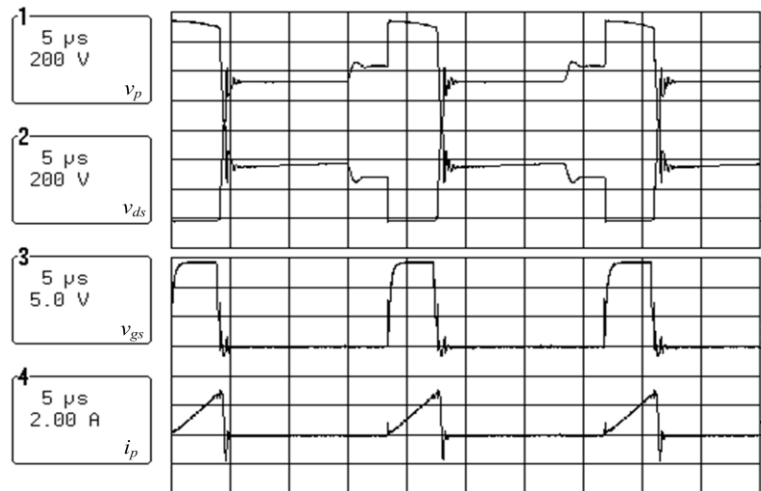


Figure 7 The Experimental Waveforms of the Key Parts of the proposed Converter at a Switching Frequency Scale

6. Concluding Remarks

In this paper, a single-stage LED converter with high power factor was presented. The proposed converter simplifies the power topology using a single-stage converter that merges a DC-DC boost converter and flyback converter, using this architecture we can also simplify its control circuit. The control of the proposed converter uses the CCM technique and the fixed on-time voltage control technique. The proposed converter has good performances in terms of high power factor, high efficiency, cost-effectiveness, and constant output voltage/current. In this paper, an operational principle and a prototype design example of the proposed converter were described, briefly, and experimental results of the prototype are shown. A 32-W prototype converter has been built based on the design example and tested to show the feasibility of the proposed converter. The prototype has shown very good performance.

Acknowledgements

This work was supported by the Soonchunhyang University Research Fund.

References

- [1] M. Doshi and R. Zane, "IEEE Trans. Power Elec.", vol. 25 (2010), pp 7.
- [2] B. Lee, H. Kim and C. Rim, "IEEE Trans. Power Elec.", vol. 26 (2011), pp12 .
- [3] Y. T. Hsieh, B. D. Liu, J. F. Wu and C. L. Fang *et.al.*, "IEEE Trans. Power Elec.", vol. 27 (2012), pp11.
- [4] C. S. Moo, Y. J. Chen and W. C. Yang, "IEEE Trans. Power Elec.", vol. 27, (2012), pp11.
- [5] S. W. Lee and S. Y. Kim, "Int. Jour. of Multimedia and Ubiquitous Engineering", vol. 2, no. 7 (2012).
- [6] N. Chen and H. S. H. Chung, "IEEE Trans. Power Elec.", vol. 5, no. 28, (2013).
- [7] K. Lee, D. Cha and K. Lee, Int. Jour. of Control and Automation, vol. 2, no. 6, (2013).
- [8] J. J. Kang, K. Um, S Yoo and G. S. Choi, *et.al.*, "Int. Jour. of Control and Automation", (2013), pp 2, 6.
- [9] X. Xie, M. Ye, Y. Cai and J. Wu, "Proceedings of IEEE Applied Power Electronic Conference and Exposition", Fort Worth, U.S.A., (2011) March 6-11.
- [10] P. Athalye, M. Harris and G. Negley, "Proceedings of IEEE Applied Power Electronic Conference and Exposition", Orlando, USA, (2012) March 5-9.
- [11] M. Arias, M. F. Diaz, D. G. Lamar, D. Balocco *et.al.*, " IEEE Trans. Power Elec.", vol. 5, no. 28, (2013).
- [12] C. S. Moo, K. H. Lee, H. L. Cheng and W. M. Chen, "IEEE Trans. Ind. Electron", vol. 4, no. 56, (2009).
- [13] D. Gacio, J. M. Alonso, A. J. Calleja, J. García *et.al.*, "IEEE Trans. Ind. Electron", vol. 2, no. 58, (2011).

- [14] Y. C. Li and C. L. Chen, "IEEE Trans. Ind. Electron", vol. 2, no. 59, (2012).
- [15] Xie, J. Wang, C. Zhao, Q. Lu and S. Liu, "IEEE Trans. Power Elec.", vol. 11, no. 27, (2012).
- [16] S. C. Moon, G. B. Koo and G. W. Moon, "IEEE Trans. Power Elec.", vol. 8, no. 28, (2013).
- [17] K. H. Liu and Y. L. Lin, "In Proceeding of the IEEE Power Electronics Specialists Conference '89", Milwaukee, U.S.A., (1989) June 26-29.

Authors



Geun-Yong Park

Geun-Yong Park received his B.S. degree in Electronic Information Engineering in 2013 from Soonchunhyang University, Korea, where he is currently working toward the M.S. degree. His research interests include DC-DC power converter, AC-DC high frequency inverter, and power conversion for the renewable energy.



Gang-YoulJeong

Gang-YoulJeong received his B.S. degree in Electrical Engineering from Yeungnam University, Korea, in 1997, and his M.S. and Ph.D. degrees in Electronic and Electrical Engineering from POSTECH (Pohang University of Science and Technology), Korea, in 1999 and 2002, respectively. He has been an associate professor in Department of Electronic Information Engineering, SoonchunhyangUniversity, Korea. His research interests include DC-DC power converter, AC-DC high frequency inverter, and power conversion for the renewable energy.